ELSEVIER

SCIENCE DIRECT®

PHYSICS LETTERS B

Physics Letters B 549 (2002) 101–108

www.elsevier.com/locate/npe

Parton percolation and J/ψ suppression

S. Digal, S. Fortunato, P. Petreczky, H. Satz

Fakultät für Physik, Universität Bielefeld, D-33501 Bielefeld, Germany

Received 26 July 2002; received in revised form 4 September 2002; accepted 4 October 2002

Editor: P.V. Landshoff

Abstract

The geometric clustering of partons in the transverse plane of nuclear collisions leads for increasing A or $\sqrt{s}$ to percolation. In the resulting condensate, the partons are deconfined but not yet in thermal equilibrium. We discuss quarkonium dissociation in this precursor of the quark–gluon plasma, with an onset of dissociation when the saturation scale of the parton condensate reaches that of the given quarkonium state.

Statistical QCD predicts color deconfinement for sufficiently hot strongly interacting systems in full equilibrium. In the resulting quark–gluon plasma, both the momenta and the relative abundances of quarks, antiquarks and gluons are determined by the temperature of the medium. It is not evident if and at what evolution stage high energy nuclear collisions produce such equilibrium, nor is it evident that color deconfinement is restricted to such ideal thermal systems. It thus seems natural to ask what conditions are necessary in the pre-equilibrium stage to achieve deconfinement and perhaps subsequent quark–gluon plasma formation. In recent years, the occurrence of color deconfinement in nuclear collisions without assuming prior equilibration has therefore been addressed on the basis of two closely related concepts, parton percolation [1,2] and parton saturation [3–5].

Both start from the observation that in a central nucleus–nucleus collision at high energy, one finds in the transverse nuclear plane interacting partons[1] of different transverse scales. At low densities, one can define individual partons originating from nucleons of the incident nuclei. Once the density of partons becomes so high that they form a dense interacting cluster, independent parton existences and origins are no longer meaningful: the resulting cluster forms a condensate of deconfined partons. The condensate is formed in the sense of droplets condensing to form a liquid, and the partons which make up this condensate are no longer constrained by any hadronic conditions.

Consider a distribution of partons of transverse size πr^2 over the transverse nuclear plane πR_A^2, with $r \gg R_A$.[2] The fundamental aim of parton percolation

E-mail address: satz@serv1.physik.uni-bielefeld.de (H. Satz).

[1] A relation between deconfinement and percolation was suggested quite long ago [6]; but the first work on color percolation in nuclear collisions was given in terms of strings [1], rather than partons. We shall nevertheless restrict ourselves here to a parton picture [2].

[2] For simplicity, we assume the partons to have a fixed transverse radius; the extension to a distribution of radii is straightforward and does not change the picture.

0370-2693/02
PII: S0370-2693(02)02782-X

studies [1,2,6] is the determination of the transition from a normal hadronic collision situation of disjoint partonic 'discs' to a connected cluster of such discs spanning the nucleus, the parton condensate. Percolation theory predicts this transition to occur when

$$\frac{N_q}{\pi R_A^2}\pi r^2 = n_q \pi r^2 \equiv \eta \to \eta_c = 1.128, \tag{1}$$

i.e., when the parton density $\eta = n_q \pi r^2$ measured in terms of parton size reaches the percolation threshold η_c. In the 'thermodynamic' limit of infinite spatial size $R_A \to \infty$ and infinite parton number $N_q \to \infty$, the largest connected cluster first spans the system at this point. The critical value $\eta_c = 1.128$ is determined by extensive numerical studies [7]. Since the partons overlap, this does not mean that the entire transverse nuclear surface is covered by parton discs. In fact, at the percolation point, only the fraction $1 - \exp(-\eta_c) \simeq 2/3$ of the nuclear area is covered by partons. At $\eta = \eta_c$, the critical clustering behavior of the system can be specified in the usual way in terms of critical exponents. In particular, the size $S(\eta)$ of the largest cluster diverges for $\eta \to \eta_c$ as

$$S(\eta) \sim (\eta_c - \eta)^{-\gamma}, \tag{2}$$

with the critical exponent $\gamma = 43/18$ [8]. While this holds strictly only for infinite systems, it is verified that even for rather small spatial systems, the transition from very small size to percolating cluster occurs in a very narrow density interval. In other words, even at finite size there is almost critical behavior. This will become quite important for our further considerations.

The essential idea of parton saturation is that the increase in the number of partons for small x, as obtained from deep inelastic scattering experiments, must stop when the density of partons becomes so high that they overlap and form large interacting clusters; fusion and splitting then causes their number to approach a constant. The onset of saturation has been discussed in various ways; making use of their transverse size, it can also be quite naturally determined by the percolation condition (1), which then fixes the saturation scale in terms of A and c.m.s energy $\sqrt{s}$. Saturation sets in when the parton density n_q in terms of the partonic interaction cross section σ_q approaches the critical value $\eta_c = 1.128$. The partonic cross section depends on its inverse transverse momentum k_T, $\sigma_g(k_T) \sim 1/k_T^2$, and the parton density $n_g(k_T^2)$ for a fixed resolution scale k_T^2 can be obtained from the gluon distribution function determined in deep inelastic scattering. The novel aspect from the point of view of percolation is that the density of partons $n_q(k_T^2)$ is related to their transverse size $\sigma(k_T^2)$, so that with the functional form of these two quantities given, the percolation condition specifies the transverse momentum scale of the percolating partons. Let us consider this in more detail.

The distribution of partons in an incident nucleon of momentum p is given in terms of their fractional momentum $x \simeq k/p$ and the resolution scale Q^2, through integration over the partonic transverse momentum k_T. The relevant resolution scale in a nucleon–nucleon collision is the largest transverse momentum $k_T^{\max} = Q$ for which partons are resolved. The number of partons at fixed x and integrated over $k_T \leqslant Q$ is given by the sum of the contributions of gluons plus those of sea quarks and antiquarks,

$$\frac{dN_q(x, Q^2)}{dy} = xg(x, Q^2) + \sum_i \Big[xq_i(x, Q^2) + x\bar{q}_i(x, Q^2) \Big], \tag{3}$$

where $g(x, Q^2)$ denotes the gluon distribution function, $q_i(x, Q^2)$ and $\bar{q}_i(x, Q^2)$ that of up and down ($i = 1, 2$) quarks and antiquarks, respectively. The distribution functions are determined from parametrisations of deep inelastic scattering data, and thus Eq. (3) provides the number of partons at central rapidity $y = 0$, with $x = Q/\sqrt{s}$. With increasing energy, the gluons become dominant; however, we shall see shortly that at SPS energy quarks and antiquarks make up about half of all partons, and even at RHIC they still constitute nearly a third of the total.

We further need the average parton size. In the simple percolation approach which we shall follow here, this is assumed to be the geometric cross section π/Q^2 for gluons as well as for quarks/antiquarks. At very high energy, more dynamical considerations (see [3–5]) lead for gluons to the same geometric form, but with some numerical modifications: $\sigma_g(Q^2) = \kappa \alpha_s(Q^2)\pi/Q^2$, where $\alpha_s(Q^2)$ is the running coupling at scale Q^2 and κ a given constant. For SPS and RHIC energies, where the transverse size for quarks and antiquarks as well as for gluons is needed, there exists

so far no comparable dynamical form. We therefore use the geometric cross section and thus obtain that in an AA collision at $y = 0$, the equation

$$n_s(A)\left(\frac{dN_q(x, Q_s^2)}{dy}\right)_{x=Q_s/\sqrt{s}} \frac{\pi}{Q_s^2} = \eta_c, \tag{4}$$

determines the value $Q = Q_s(A, \sqrt{s})$ at the onset of percolation. Here $n_s(A)$ specifies the density of parton sources in the transverse plane of a central AA collision. At SPS energy $\sqrt{s} \simeq 20$ GeV, this is essentially the density of wounded nucleons [9], $n_s(A) \simeq n_w(A)$. For higher energies and harder partons, collision-dependent contributions will play a significant role, and so a more suitable form here is a combination of the two sources,

$$n_s(A) = (1 - \bar{x})n_w + \bar{x}n_{\rm coll}, \tag{5}$$

with $0 \leqslant \bar{x} \leqslant 1$ [10].

As determined by Eq. (4), partons with $k_T \leqslant Q_s$ condense to form an overlapping and hence interacting cluster spanning the system, the parton condensate. Within this cluster, they can fuse or split and thus lose their independent existence. We recall that at this point, 2/3 of the nuclear area is covered by the parton condensate.

The relation between saturation and percolation has so far not been much emphasized. For a study of the new percolating medium at very large A or $\sqrt{s}$, the 'color glass condensate' of Ref. [5], it is indeed not so important. However, it does become crucial for a detailed picture of the onset of parton condensation. We know from percolation theory that in the large volume limit this is a critical phenomenon and hence even for finite systems takes place in an almost singular way.

To study the onset of parton percolation in AA collisions, it is convenient to rewrite Eq. (4) in the form

$$\frac{1}{Q_s^2}\left(\frac{dN_q(x, Q_s^2)}{dy}\right)_{x=Q_s/\sqrt{s}} = \frac{25\eta_c}{\pi n_s(A)} \simeq \frac{8.98}{n_s(A)}, \tag{6}$$

with the density of parton sources n_s in fm^{-2}; the factor 25 arises when this is converted to GeV$_2$. In Eq. (6), the hadronic parton distribution $(dN_q/dy)/Q^2$ is compared to the density of parton sources in a nucleus–nucleus collision. For low source densities, i.e., for small A, $8.98/n_s(A)$ remains well above the A-independent l.h.s., which is a function only of Q and $\sqrt{s}$: there are not enough partons to form a condensate. For sufficiently large A, however, $8.98/n_s(A)$ intersects $(dN_q/dy)/Q^2$ at some Q_s, thus defining the onset of percolation. The condensate contains all partons with $k_T \leqslant Q_s$; parton interactions now prevent much further increase in number, i.e., there is saturation.

To see when that happens, we have to make use of a specific set of parton distribution functions. The kinematic range relevant for our analysis is 0.5 GeV$^2 < Q^2 < 2$ GeV^2, with $0.02 \leqslant x < 0.1$ for SPS and $0.003 < x < 0.02$ for RHIC. Among the commonly used PDF parametrizations, only the set GRV94 [11] goes down to such small values of Q^2. This parametrization describes well the available data on the proton structure function F_2^p from the E665 and NMC Collaborations for 0.4 GeV$^2 < Q^2 < 2$ GeV^2 and $x < 0.01$ [12,13]. It also reproduces quite well the small x HERA data [11,14] for $x > 10^{-3}$. We have therefore calculated (dN_q/dy) using the next-to-leading order GRV94 PDFs in the DIS scheme (GRV94DI) [11]; the resulting $(dN_q/dy)/Q^2$ curves are shown in Figs. 1(a) and (b) for SPS (20 GeV) and RHIC (200 GeV) c.m.s. energies, respectively.

The uncertainty in (dN_q/dy) is mainly due to the gluon distribution. At SPS energy, this can be estimated by comparing calculations using leading and next-to-leading order GRV94 PDFs. The resulting uncertainty is below 3% for $Q^2 > 0.6$ GeV^2 and increases to at most 10% at 0.5 GeV^2. At RHIC, the next-to-leading order GRV94 PDF's are consistent with the gluon distributions determined by the H1 and ZEUS Collaborations and with the constraints from charm measurements [15], while the leading order results for the gluon distribution are too large. This gives us some confidence in using the next-to-leading order GRV94 parametrization.

We also note that these gluon distributions are not very different from those proposed in more recent phenomenological saturation studies for $x < 0.01$ [16]. This approach is very successful in describing the low x HERA data and it can in fact also account for the E665 data on F_2^p in the kinematical region relevant for RHIC. The gluon distribution of [16] is directly related to F_2^p; the sea quarks are present only virtually as small dipoles from photon splitting [17]. In such an approach, the uncertainty in the gluon distribution

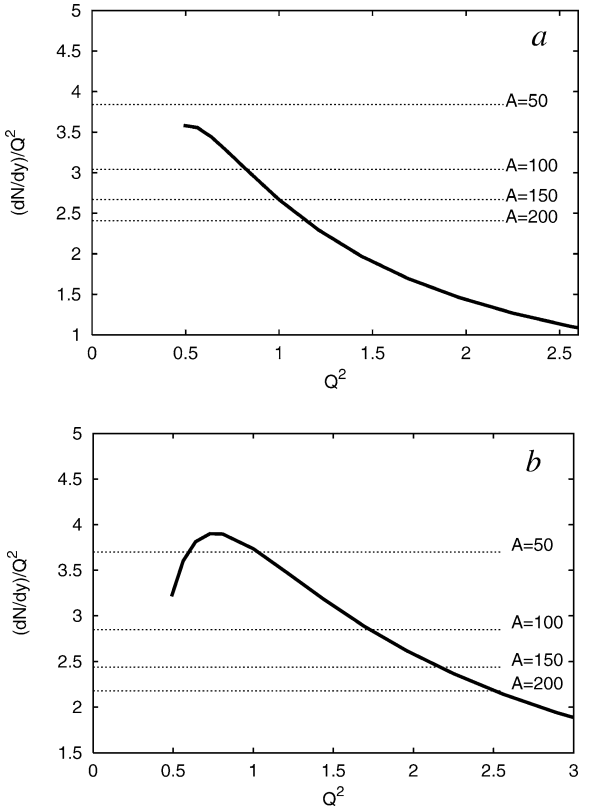

Fig. 1. Parton distribution vs. Q^2 (in GeV^2), with the percolation limits obtained for different central AA collisions: (a) $\sqrt{s} = 20$ GeV, (b) $\sqrt{s} = 200$ GeV.

can be avoided, and it has been used to predict the $\sqrt{s}$-dependence of hadron multiplicities at RHIC [18].

Once the density of the percolating medium is sufficiently high, the PDF approach of Ref. [16] to the gluon distribution is more appropriate to study the resulting condensate; however, it is not suitable to study the onset of condensation. In this connection we note that the effect of the sea quarks cannot be completely neglected even at RHIC energy. In general, the relative weight of the different parton species in the produced condensate will depend on Q and $\sqrt{s}$, and with increasing energy, the condensate becomes more and more gluon-dominated. Thus the ratio of gluons to quarks and antiquarks in the parton condensate based on the GRV94 PDFs is at $Q = 1$ GeV found to be about 1 for SPS energy and 2 for RHIC; in a chemically equilibrated quark–gluon plasma, it is about 1/2. Hence before thermalization, the medium

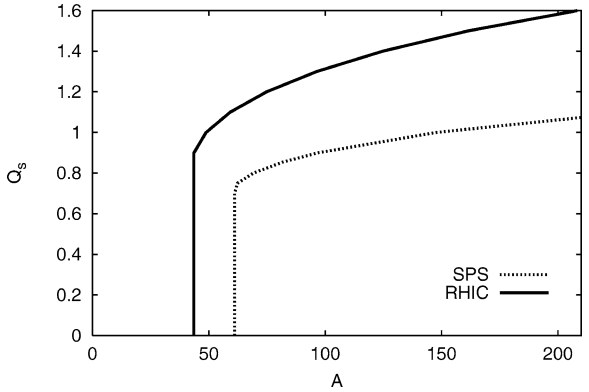

Fig. 2. Saturation momenta Q_s (in GeV) vs. A for central AA collisions at SPS and RHIC energies.

contains more than the equilibrium share of gluons [20], and this gluon dominance increases with energy.

In order to illustrate the effect for different central AA collisions, we assume a spherical nuclear profile, which gives at SPS energy, with $x = 0$ in Eq. (5),

$$n_s(A) = n_w(A) = \frac{2A}{\pi A^{2/3}}. \tag{7}$$

Inserting this into Eq. (6), together with the values of $[dN_q(x, Q^2)/dy]/Q^2$ at $\sqrt{s} = 20$ GeV determined above, we obtain the results shown in Fig. 1(a). The intersection points determine the onset of percolation. This very simplified picture shows that parton condensation begins for $A \simeq 60$, with $Q \simeq 0.7$ GeV. To obtain the corresponding behavior at $\sqrt{s} = 200$ GeV, nucleon collisions have to be included as source of partons. With

$$n_{\text{coll}} = \frac{3}{4}\left(\frac{A^{4/3}}{\pi A^{2/3}}\right); \tag{8}$$

and $x = 0.09$ [10] in Eq. (5), we find the percolation points in Fig. 1(b). In Eq. (8), the factor 3/4 comes from averaging over the nuclear profile. In Fig. 2, the percolation values Q_s for central AA collisions are displayed as function of A. At SPS energy, we thus do not obtain parton condensation below $A \simeq 60$; at RHIC energy, the higher parton density lowers the onset to $A \simeq 40$.

In the experimental study of J/ψ suppression, the production is measured at different centralities, so that we now have to determine the parton source density at fixed A and varying impact parameter. This is done in a Glauber analysis based on Woods–Saxon

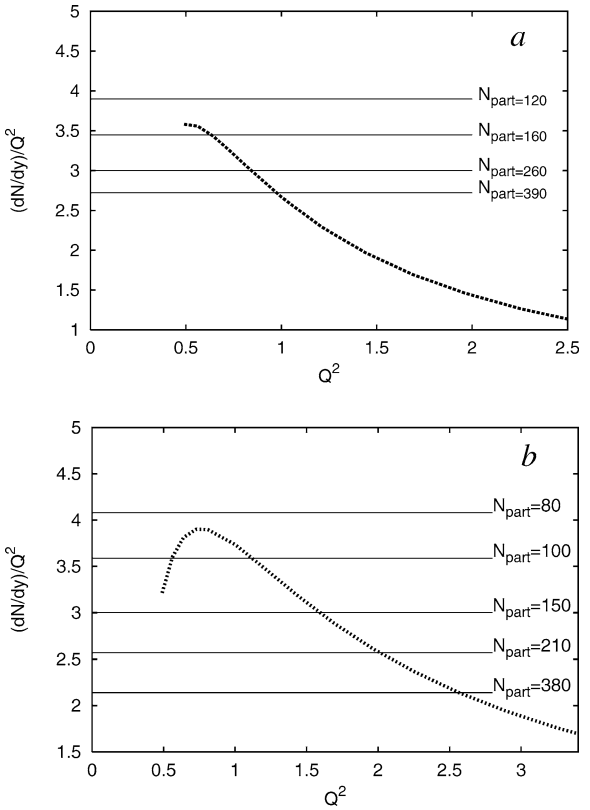

Fig. 3. Parton distribution vs. Q^2 (in GeV^2), with the percolation limits for different centralities, given by the number of participant nucleons: (a) Pb–Pb at $\sqrt{s} = 20$ GeV, (b) Au–Au at $\sqrt{s} = 200$ GeV.

nuclear profiles, with a collision-determined weight [19]. In Fig. 3(a), we show the resulting percolation behavior as function of the effective number $N_{\rm part}$ of participants in a Pb–Pb collision at $\sqrt{s} = 20$ GeV. The threshold for parton percolation is found to be slightly below $N_{\rm part} \simeq 150$. The corresponding calculations for Au–Au collisions at $\sqrt{s} = 200$ GeV, with a collision-dependent term in n_s and again $x = 0.09$ in Eq. (5), lead to the results shown in Fig. 3(b). The onset of parton condensation at RHIC is thus shifted to considerably more peripheral collisions. In Fig. 4, the centrality dependence of the percolation scale Q_s is shown; at the onset point, the condensate contains partons of different sizes r, with $r \geqslant 1/(0.7\ \text{GeV})$ at SPS and $r \geqslant 1/(0.9\ \text{GeV})$ at RHIC.

We now turn to the effect of parton condensation on J/ψ production. It is known from pA collisions that normal nuclear matter leads to reduced charmonium

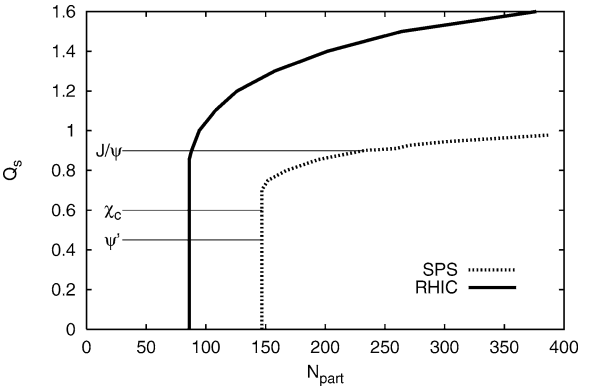

Fig. 4. Saturation momenta Q_s vs. $N_{\rm part}$ for central Pb–Pb collisions at $\sqrt{s} = 20$ GeV and central Au–Au collisions at $\sqrt{s} = 200$ GeV, together with the critical scales for anomalous J/ψ, χ_c and ψ' suppression.

production. Therefore, we first have to consider such 'normal' suppression, since for pA collisions, at least up to RHIC energies, we are well below the threshold for parton condensation.[3] Consider the production of charmonium in the nuclear target rest frame. A gluon from the incident proton fluctuates into a virtual $c\bar{c}$ pair; in a collision with one of the target nucleons this is brought on-shell, its color is neutralized, and it eventually becomes a physical J/ψ of size $d_{J/\psi} \simeq 0.4$ fm. Thus in the rest-frame of the $c\bar{c}$ pair, a time of at least 0.4 fm is needed for J/ψ formation. During its pre-resonance stage, for $\tau_{c\bar{c}} \leqslant 0.4$ fm, it will travel a distance

$$d_{c\bar{c}} = \tau_{c\bar{c}} \frac{s x_F}{4Mm} \left[1 + \sqrt{1 + \frac{4M^2}{s x_F^2}} \right] \tag{9}$$

in the target rest frame; here m denotes the mass of the nucleon, M that of the $c\bar{c}$ pair and x_F the $c\bar{c}$ Feynman momentum fraction. For the production of a $c\bar{c}$ at rest in the nucleon–nucleon c.m.s., this becomes $d_{c\bar{c}} = \tau_{c\bar{c}}(\sqrt{s}/2m)$. From this it is immediately seen that at $\sqrt{s} \simeq 40$ GeV, and $x_F \geqslant 0$, the nascent J/ψ effectively traverses even heavy nuclear targets in its pre-resonance stage. The situation is very similar for χ_c and ψ' production, for which the pre-resonance

[3] A determination of the collision energy for which parton saturation occurs in $pp/p\bar{p}$ or pA collisions is presently difficult, since it involves x-values much smaller than presently accessible in deep inelastic scattering. Disregarding this small x-behavior leads to a very early onset of parton percolation [23].

life-times are if anything even larger. Thus for the mentioned $\sqrt{s}$ and x_F, the nuclear target sees of all charmonium states only the small pre-resonance precursor, so that all should suffer the same degree of nuclear suppression [21]. For negative x_F (and perhaps to some extent also for lower $\sqrt{s}$), the nucleus should begin to see physical resonances, and as a result the suppression should become larger for the higher excited states with their larger radii [22].

On the basis of this information, normal charmonium suppression has generally been studied in terms of pre-resonance dissociation in standard nuclear matter, leading to a break-up cross section around 5–6 mb [19,24]. This implies a mean free path of about 12 fm. For a multiple collision analysis of Glauber type, the mean free path has to exceed the coherence length (essentially the size) of the pre-resonance in the rest frame of the nucleus: otherwise, the $c\bar{c}$ is wounded several times before it has had a chance to register the first interaction. For collision energies $\sqrt{s} \leqslant 40$ GeV, i.e., in the range of fixed target experiments, this condition is satisfied, with coherence lengths below 8 fm. At RHIC energy, on the one hand the cross section for pre-resonance break-up in normal nuclear matter could change, and on the other hand the coherence length becomes dilated ten times more. Now interference effects of the Landau–Pomeranchuk–Migdal type may have to be taken into account, which could lead to a reduction of 'normal' nuclear suppression [25]. Hence measurements of charmonium production in pA collisions at RHIC are absolutely essential for an understanding of whatever J/ψ suppression in AA collisions is observed there.

We now want to consider the additional 'anomalous' suppression of charmonium production due to the dense partonic medium created in AA collisions. The virtual partons in the incoming nuclei coalesce to form a condensate in a time $t_c \simeq 1/Q_s$ determined by the saturation scale; in the color glass picture [5], this is the time needed to melt the frozen glass. The interacting and expanding parton condensate can subsequently lead to the formation of a thermalized quark–gluon plasma; a crucial factor for this is the energy density reached at thermalization. We restrict ourselves here to the parton condensate stage.

In AA collisions at RHIC energy, the colliding nuclei are Lorentz-contracted to about 0.1 fm in the overall c.m.s. They will therefore sweep past the nascent charmonium in its pre-resonance state and before parton condensation sets in, resulting in some form of normal nuclear absorption. After about 0.2 fm, the nuclei are well out of the way and the parton condensate is formed. Any produced and surviving charmonium states now encounter this new medium, either as fully formed resonances or in the late pre-resonance stage. For SPS energy, a similar discussion is more complex, since the nuclei are contracted to only about 1 fm diameter; this will introduce a smearing in the comparison of the different time scales. We shall here neglect this and assume that also at the SPS there is first pre-resonance absorption in normal nuclear matter, followed by the effect of the parton condensate on the survivors.

In the first attempt to describe J/ψ suppression in terms of parton percolation [2], it was assumed that different charmonium states i define particular scales Q_i, and the onset of percolation for partons of that scale leads to the dissociation of all charmonia of that species within the percolating cluster. The number of partons was taken as a scale-independent function of $\sqrt{s}$. Parton saturation in fact specifies $[dN_q/dy](Q_s^2)$ as function of the scale Q_s, so that we now have (see Figs. 2 and 4) a parameter-free determination of the onset line $Q_s(A)$ or $Q_s(N_{\rm part})$ of parton condensation at a given collision energy.

Within the parton condensate, color fields of a Q_s-dependent strength will affect the binding of a $c\bar{c}$ dipole charmonium state. This effect can be addressed in different ways. One possible way is to consider the $c\bar{c}$ propagation in a classical field, which can represent the gluon field of the condensate or that of the nucleus; the specification of the medium is encoded in the corresponding field correlator [25]. For a small singlet dipole the probability to remain singlet is proportional to $\exp(-\kappa r^2)$, where r is the dipole size and κ is a dimensional parameter determined by the field strength. In the color glass approach, $\kappa \sim Q_s^2$ [5]. Thus for small singlet dipoles, $Q_s^2 r^2 \ll 1$, the probability to remain in a singlet state is close to unity (color transparency). Motivated by this fact we shall here adopt the simple model of Ref. [2], assuming that a charmonium state i of scale Q_i will be dissociated if it finds itself in a parton condensate of scale $Q_s \geqslant Q_i$; otherwise it will survive. This very simplistic picture allows an analysis of nuclear profile effects (condensed and non-condensed regions of the colli-

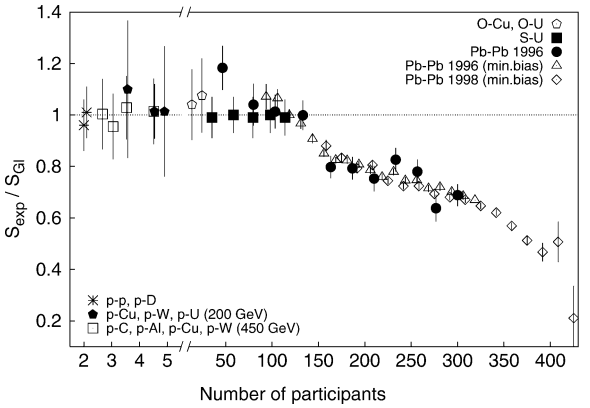

Fig. 5. The J/ψ survival probability determined at SPS energy as function of the number of participant nucleons, from [29].

sion profile) and thus provides some direct predictions for the centrality-dependence of anomalous J/ψ suppression for given A and $\sqrt{s}$. Other approaches that have been suggested include the study of the time evolution of the screening masses in the parton cascade [26] and in the color glass condensate [27].

The radii of the observable charmonium states as obtained from the solution of the Schrödinger equation with Cornell potential are [28]

$$r_{J/\psi} \simeq (0.9\ \text{GeV})^{-1}, \qquad r_{\chi} \simeq (0.6\ \text{GeV})^{-1},$$
$$r_{\psi'} \simeq (0.45\ \text{GeV})^{-1}. \tag{10}$$

These values have to be compared to the partonic saturation radii Q_s^{-1} shown in Fig. 4 as functions of the number of participants in central AA collisions. It is seen that at SPS energy, the onset of χ_c and ψ' suppression effectively coincides with the onset of parton condensation, while the J/ψ survives up to larger Q_s and higher parton densities.[4] Hence in Pb–Pb collisions, anomalous suppression should start with the elimination of J/ψ feed-down from χ_c and ψ' at $N_{\text{part}} \simeq 150$; the further suppression of direct J/ψ production should set in for $N_{\text{part}} \simeq 250$. In Fig. 5 we show the suppression pattern observed by the NA50 Collaboration at the CERN-SPS [29]; the two 'steps' observed in the anomalous suppression pattern agree fairly well with the expected onsets of parton condensation. Note that at the percolation points, the percolating cluster covers only a fraction of the transverse area; with increasing centrality, this fraction increases. The present study only indicates the onset points for suppression; more detailed studies are needed to determine the actual amount of suppression as function of centrality. In particular, one has to take into account the actual nuclear profile and determine the fraction of J/ψ produced in regions where there is no percolation, since this fraction will survive (see [2]). Work on this is in progress; it corresponds to identifying "hot" and "cold" regions in QGP suppression studies [30].

Finally we want to consider the suppression pattern expected for RHIC experiments. From Fig. 4, it is seen that for $N_{\text{part}} \geqslant 80$, all charmonium states should suffer anomalous suppression, so that here there should only be one onset point. Moreover, collisions with $N_{\text{part}} = 80$ correspond to an impact parameter of $b \simeq 10$ fm, and this may be too peripheral for meaningful measurements. For a study of the onset of anomalous suppression at RHIC, it will thus most likely be necessary to study AA collisions for much lower A, as already noted previously [2].

In conclusion, we have shown that a very simple parton percolation approach leads to a conceptually reasonable description of the observed anomalous J/ψ suppression pattern. In particular, it is seen that this suppression can arise from pre-equilibrium deconfinement alone, without any thermalization. On the other hand, it should be emphasized that the present study can only give a qualitative illustration of the main consequences of the approach; it is clear that uncertainties in parton distributions and transverse sizes lead to corresponding uncertainties in the specific values of the onset points.

Acknowledgements

It is a pleasure to thank D. Kharzeev and M. Nardi for their contribution to an early version of this study [2] as well as for many helpful discussions and comments.

[4] The fate of the ψ' is most likely more complex. It should certainly be dissociated once parton condensation sets in; however, it is very much more weakly bound than the χ_c and J/ψ states, so that a less dense environment could also lead to its break-up.

References

[1] N. Armesto, et al., Phys. Rev. Lett. 77 (1996) 3736;
M. Nardi, H. Satz, Phys. Lett. B 442 (1998) 14.
[2] D. Kharzeev, M. Nardi, H. Satz, Nucl. Phys. A 661 (1999) 104c.
[3] L.V. Gribov, E.M. Levin, M.G. Ryskin, Phys. Rep. 100 (1983) 1;
A.H. Mueller, J. Qiu, Nucl. Phys. B 268 (1986) 427;
J.-P. Blaizot, A.H. Mueller, Nucl. Phys. B 289 (1987) 847.
[4] L. McLerran, R. Venugopalan, Phys. Rev. D 49 (1994) 2233;
L. McLerran, R. Venugopalan, Phys. Rev. D 49 (1994) 3352;
L. McLerran, R. Venugopalan, Phys. Rev. D 50 (1994) 2225.
[5] E. Iancu, A. Leonidov, L. McLerran, Nucl. Phys. A 692 (2001) 583;
E. Ferreiro, E. Iancu, A. Leonidov, L. McLerran, Nucl. Phys. A 703 (2002) 489;
L. McLerran, in: Lecture Notes in Physics, Vol. 583, Springer, Berlin, 2002, p. 291, hep-ph/0104285;
D. Kharzeev, hep-ph/0204014, and references therein.
[6] G. Baym, Physica 96A (1979) 131;
T. Çelik, F. Karsch, H. Satz, Phys. Lett. B 97 (1980) 128;
For an update, see H. Satz, Nucl. Phys. A 642 (1998) 130c.
[7] E.T. Gawlinski, H.E. Stanley, J. Phys. A 10 (1977) 205.
[8] See, e.g., M.S. Isichenko, Rev. Mod. Phys. 64 (1992) 961.
[9] M.C. Abreu, et al., NA50 Collaboration, Phys. Lett. B 530 (2002) 43.
[10] D. Kharzeev, M. Nardi, Phys. Lett. B 507 (2001) 121.
[11] M. Glück, E. Reya, A. Vogt, Z. Phys. C 67 (1995) 433.
[12] M.R. Adams, et al., E665 Collaboration, Phys. Rev. D 54 (1996) 3006.
[13] M. Arneodo, et al., NMC Collaboration, Nucl. Phys. B 483 (1997) 3.
[14] M. Glück, E. Reya, A. Vogt, Eur. Phys. J. C 5 (1998) 461.
[15] K. Nagano, H1, ZEUS Collaboration, J. Phys. G 28 (2002) 737.
[16] K. Golec-Biernat, M. Wüsthof, Phys. Rev. D 59 (1999) 014017;
K. Golec-Biernat, M. Wüsthof, Phys. Rev. D 60 (1999) 114023;
K. Golec-Biernat, M. Wüsthof, Eur. Phys. J. C 20 (2001) 313.
[17] A.H. Mueller, Nucl. Phys. B 558 (1999) 285.
[18] D. Kharzeev, E. Levin, Phys. Lett. B 523 (2001) 79.
[19] D. Kharzeev, et al., Z. Phys. C 74 (1997) 307.
[20] E.V. Shuryak, Phys. Rev. Lett. 68 (1992) 3270.
[21] D. Kharzeev, H. Satz, Phys. Lett. B 366 (1996) 316.
[22] D. Kharzeev, H. Satz, Phys. Lett. B 356 (1995) 365.
[23] J. Dias de Deus, A. Rodrigues, hep-ph/0205253.
[24] R. Shahoyan, NA50 Collaboration, Presentation at the XXVII Rencontre de Moriond, Les Arcs, France, 16–23 March, 2002.
[25] H. Fujii, T. Matsui, nucl-th/0204065;
H. Fujii, nucl-th/0205066.
[26] H. Satz, D.K. Srivastava, Phys. Lett. B 475 (2000) 225.
[27] V.P. Gonçalves, Phys. Lett. B 518 (2001) 79.
[28] F. Karsch, M.-T. Mehr, H. Satz, Z. Phys. C 37 (1988) 617;
F. Karsch, H. Satz, Z. Phys. C 51 (1991) 209.
[29] M.C. Abreu, et al., NA50 Collaboration, Phys. Lett. B 477 (2000) 28;
M.C. Abreu, et al., NA50 Collaboration, Phys. Lett. B 521 (2001) 195;
M. Nardi, private communication.
[30] S. Gupta, H. Satz, Phys. Lett. B 283 (1992) 439;
J.-P. Blaizot, J.-Y. Ollitrault, Phys. Rev. Lett. 77 (1996) 1703.